

DRY MERGERS IN GEMS: THE DYNAMICAL EVOLUTION OF MASSIVE EARLY-TYPE GALAXIES

ERIC F. BELL,¹ THORSTEN NAAB,² DANIEL H. MCINTOSH,³ RACHEL S. SOMERVILLE,⁴ JOHN A. R. CALDWELL,⁵
MARCO BARDEN,¹ CHRISTIAN WOLF,⁶ HANS-WALTER RIX,¹ STEVEN V. BECKWITH,^{4,7} ANDREA BORCH,⁸
BORIS HÄUSSLER,¹ CATHERINE HEYMANS,^{1,9} KNUD JAHNKE,¹⁰ SHARDHA JOGEE,¹¹ SERGEY KOPOSOV,¹
KLAUS MEISENHEIMER,¹ CHIEN Y. PENG,⁴ SEBASTIAN F. SANCHEZ,¹² AND LUTZ WISOTZKI⁹

Received 2005 June 17; accepted 2005 November 18

ABSTRACT

We have used the $28' \times 28'$ *Hubble Space Telescope* image mosaic from the GEMS (Galaxy Evolution from Morphology and SEDs) survey in conjunction with the COMBO-17 photometric redshift survey to constrain the incidence of major mergers between spheroid-dominated galaxies with little cold gas (dry mergers) since $z = 0.7$. A set of N -body merger simulations was used to explore the morphological signatures of such interactions: they are recognizable either as <5 kpc separation close pairs or because of broad, low surface brightness tidal features and asymmetries. Data with the depth and resolution of GEMS are sensitive to dry mergers between galaxies with $M_V \lesssim -20.5$ for $z \lesssim 0.7$; dry mergers at higher redshifts are not easily recovered in single-orbit *HST* imaging. Six dry mergers (12 galaxies) with luminosity ratios between 1 : 1 and 4 : 1 were found from a sample of 379 red early-type galaxies with $M_V < -20.5$ and $0.1 < z < 0.7$. The simulations suggest that the morphological signatures of dry merging are visible for ~ 150 Myr, and we use this timescale to convert the observed merger incidence into a rate. On this basis we find that present-day spheroidal galaxies with $M_V < -20.5$ on average have undergone between 0.5 and 2 major dry mergers since $z \sim 0.7$. We have compared this result with the predictions of a cold dark matter–based semianalytic galaxy formation model. The model reproduces the observed declining major merger fraction of bright galaxies and the space density of luminous early-type galaxies reasonably well. The predicted dry merger fraction is consistent with our observational result. Hence, hierarchical models predict and observations now show that major dry mergers are an important driver of the evolution of massive early-type galaxies in recent epochs.

Subject headings: galaxies: elliptical and lenticular, cD — galaxies: evolution — galaxies: general — galaxies: interactions — galaxies: structure

1. INTRODUCTION

Numerical simulations have long predicted that early-type galaxies, with spheroid-dominated stellar light profiles, are a natural outcome of major galaxy mergers (e.g., Toomre & Toomre 1972; Barnes & Hernquist 1996; Naab & Burkert 2003). Yet, both the timing and nature of the violent assembly of early-type galaxies remain frustratingly unclear. Look-back studies have recently become large enough to demonstrate a steady growth

in the total stellar mass in the red-sequence galaxy population since $z \sim 1$ (e.g., Chen et al. 2003; Bell et al. 2004b; Faber et al. 2006). The majority of these red-sequence galaxies are morphologically early type out to at least $z \sim 0.7$ (Bell et al. 2004a); indeed, recent works have confirmed a growth in the total stellar mass in morphologically early-type galaxies from $z \sim 1$ to the present day (Cross et al. 2004; Conselice et al. 2005). This growth is dominated by a growing number of $\sim 0.5-2L^*$ early-type galaxies (e.g., Bell et al. 2004b; Drory et al. 2004; Faber et al. 2006).¹³ Interestingly, relatively few blue galaxies bright enough to be the star-forming progenitor of a massive non-star-forming early-type galaxy are observed (Bell et al. 2004b; Faber et al. 2006). Thus, it has been suggested that mergers between non-star-forming early-type galaxies may occur (so-called “dry mergers”) and build up the massive early-type galaxy population (Bell et al. 2004b; Faber et al. 2006). Such mergers are observed at least in clustered environments (van Dokkum et al. 1999; Tran et al. 2005). Yet, it is still unclear how important dry mergers are in driving the evolution of luminous, massive early-type galaxies, averaged over all cosmic environments.

Dry mergers may also play an important role in explaining another interesting phenomenon: the strong differences between the observed properties of high-luminosity (with $M_V \lesssim -21$) and low-luminosity early-type galaxies. Luminous (i.e., massive) early-type galaxies possess boxy isophotes, cores in their light distributions, and are supported primarily by random stellar

¹ Max-Planck-Institut für Astronomie, Königstuhl 17, D-69117 Heidelberg, Germany; bell@mpia.de.

² Universitäts-Sternwarte München, Scheinerstrasse 1, D-81679 Munich, Germany.

³ Department of Astronomy, University of Massachusetts, 710 North Pleasant Street, Amherst, MA 01003.

⁴ Space Telescope Science Institute, 3700 San Martin Drive, Baltimore, MD 21218.

⁵ University of Texas, McDonald Observatory, Fort Davis, TX 79734.

⁶ Department of Physics, Denys Wilkinson Building, University of Oxford, Keble Road, Oxford OX1 3RH, UK.

⁷ The Johns Hopkins University, 9400 North Charles Street, Baltimore, MD 21218.

⁸ Astronomisches Rechen-Institut, Mönchhofstrasse 12-14, D-69120 Heidelberg, Germany.

⁹ Department of Physics and Astronomy, University of British Columbia, 6224 Agricultural Road, Vancouver, BC V6T 1Z1, Canada.

¹⁰ Astrophysikalisches Institut Potsdam, An der Sternwarte 16, D-14482 Potsdam, Germany.

¹¹ Department of Astronomy, University of Texas at Austin, 1 University Station, C1400, Austin, TX 78712-0259.

¹² Centro Astronomico Hispano Aleman de Calar Alto, Calle Jesus Durban Remon 2-2, E-04004 Almeria, Spain.

¹³ Although it is possible that the number of very massive galaxies, with $L > 5L^*$, does not change by a large amount since $z \sim 1.5$ (e.g., Saracco et al. 2005).

motions. In contrast, faint early-type galaxies have diskier isophotes, derive more support from organized rotational motions, and have power-law (or Sérsic) light distributions all the way into their innermost regions (e.g., Bender 1988; Kormendy & Bender 1996; Lauer et al. 1995; Faber et al. 1997; Graham 2004). These structural differences may be the results of galaxy merging between different types of progenitors (Khochfar & Burkert 2003).

There is growing evidence that the faint early-type galaxy population has grown substantially at recent times through galaxy merging and/or disk fading. There is a deficit of faint red-sequence galaxies in $z \sim 1$ galaxy clusters (Kodama et al. 2004; de Lucia et al. 2004), and those that are present appear to have rather young stellar populations (van der Wel et al. 2004). Furthermore, faint early-type galaxies at the present day can have important contributions from younger stars (Kuntschner 2000; Trager et al. 2000; Thomas et al. 2005). Simulations of merging disks easily yield remnants with properties consistent with the typically disky, partially rotationally supported low-luminosity elliptical galaxies (e.g., Toomre & Toomre 1972; Naab et al. 1999; Bendo & Barnes 2000; Naab & Burkert 2003), especially for unequal-mass interactions. Taken together with observations of a declining merger rate, implying between 0.2 and 1 merger per L^* galaxy (e.g., Le Fèvre et al. 2000; Patton et al. 2002; Conselice et al. 2003, although see Lin et al. 2004), it is likely that mergers between gas-rich galaxies have played an important role in building up low-luminosity early-type galaxies.

In contrast, it is increasingly clear that mergers of gas-rich disks cannot be the main formation route of more massive early-type galaxies. Not only are there relatively few blue star-forming galaxies at $z \lesssim 1$ luminous enough to fade into present-day massive non-star-forming galaxies, but the boxy isophotes and cores in the light distributions of massive early-type galaxies are challenging to reproduce in mergers of disk galaxies (Naab & Burkert 2001, 2003; Barnes 2002). Such properties can, however, be naturally reproduced by mergers of elliptical galaxies (Naab et al. 2006). This hypothesis is given some observational support by van Dokkum et al. (1999) and Tran et al. (2005), who found that $\sim 15\%$ of bright galaxies in the outskirts of the cluster MS 1054–03 were in bound pairs and were likely to merge on $\lesssim 1$ Gyr timescales; most of these are pairs of early-type galaxies. Semi-analytic work by Khochfar & Burkert (2003, 2005) supports the formation of massive early-type galaxies ending up in clusters by this route.

A direct measure of the frequency of dry mergers over the last half of cosmic time will further constrain the importance of this process in driving the evolution of the luminous early-type galaxy population. Furthermore, because the majority of massive galaxies are red early-type galaxies at all epochs since $z \sim 1$ (Bell et al. 2004b), the dry merger rate gives important insight into the merging history of the most massive galaxies at recent times. Finally, gas-free mergers are relatively straightforward to model, and their luminosity and color evolution is easily predicted, significantly simplifying the estimation of merger rates.

The goal of this paper is to use these data to constrain the incidence of dry mergers in the Galaxy Evolution from Morphology and SEDs (GEMS) data set. To realize this goal, a number of ingredients must be in place. First, a scheme must be devised by which one can reliably and reproducibly identify mergers of gas-poor systems. Second, the timescale over which signatures of gas-poor merging are identifiable must be characterized. Finally, these criteria must be applied to the data; coupled with the timescale, a merger frequency can be estimated.

In this paper, we present our first attempt to address this issue using high-resolution *Hubble Space Telescope* (*HST*) data from GEMS (Rix et al. 2004), photometric redshifts from Classifying Objects by Medium-Band Observations in 17 filters (COMBO-17; Wolf et al. 2004), and state-of-the-art N -body and semianalytic simulations. We briefly describe the data in § 2. We outline the selection philosophy in § 3. In order to devise criteria by which one can select candidate dry mergers and understand over which timescale these selection criteria are sensitive, we explore the characteristics of a suite of N -body simulation mergers between spheroid-dominated galaxies (§ 3.1). We then apply these selection criteria to the data in § 3.2. We use these results to derive a dry merger fraction and incidence in § 4. In § 5 we compare our results with limits on dry merger rates from other observations and with published merger rates and compare the observations with the predictions of a cold dark matter (CDM)–based semianalytic model. In the Appendix, we explore the importance of high-speed flyby (unbound) interactions and argue that the vast majority of tidally distorted interacting spheroidal galaxies should be in the lowest density environments capable of hosting spheroid-dominated galaxies and are therefore likely to merge. Throughout, we assume $\Omega_m = 0.3$, $\Omega_m + \Omega_\Lambda = 1$, and $H_0 = 70 \text{ km s}^{-1} \text{ Mpc}^{-1}$.

2. THE DATA

COMBO-17 has imaged the $\sim 30' \times 30'$ extended Chandra Deep Field–South using five broad and 12 medium passbands complete to apparent R -band magnitude limits of $m_R \sim 23.5$. Using these 17 passband photometric data in conjunction with galaxy, star, and active galactic nucleus template spectra, classifications and redshifts are assigned for $\sim 99\%$ of the objects with sufficient flux. The typical galaxy redshift accuracy is $\delta z/(1+z) \sim 0.02$ (Wolf et al. 2004), allowing construction of rest-frame colors and absolute magnitudes accurate to ~ 0.1 mag. In order to probe interactions between gas-free, non-star-forming galaxies, we select only galaxies on the red sequence with photometric redshifts $0.1 < z < 0.7$ for further study, following Bell et al. (2004b) and McIntosh et al. (2005).

We use F850LP imaging from the GEMS survey to provide $0''.07$ resolution data for our sample of red-selected galaxies. Using the Advanced Camera for Surveys (ACS; Ford et al. 2003) on the *HST*, a $\sim 28' \times 28'$ area of the Extended Chandra Deep Field was surveyed to a depth allowing galaxy detection to a limiting surface brightness of $\mu_{F850LP, AB} \sim 24 \text{ mag arcsec}^{-2}$ (Rix et al. 2004); in practice early-type galaxies have relatively high surface brightnesses and are limited only by the magnitude limit of COMBO-17 redshift classification.

3. THE SELECTION OF DRY MERGERS

For the sake of clarity, we present our selection criteria for candidate dry mergers here. Our philosophy is to catch the merging galaxies during the early stage of merging, when the two galaxy nuclei are distinct entities, allowing relatively accurate characterization of the progenitors, including, importantly, an estimate of the mass ratio of the merger.

Therefore, we select for further study very close pairs of red-sequence bulge-dominated galaxies with (1) projected separation < 20 kpc, (2) a V -band absolute magnitude difference of 1.5 mag or less (corresponding to a 4 : 1 luminosity ratio difference, our threshold for a major merger), and (3) photometric redshift difference $|\Delta z| < 0.1$.

However, not all projected close pairs will be merging; some may be projections of galaxies at significantly different

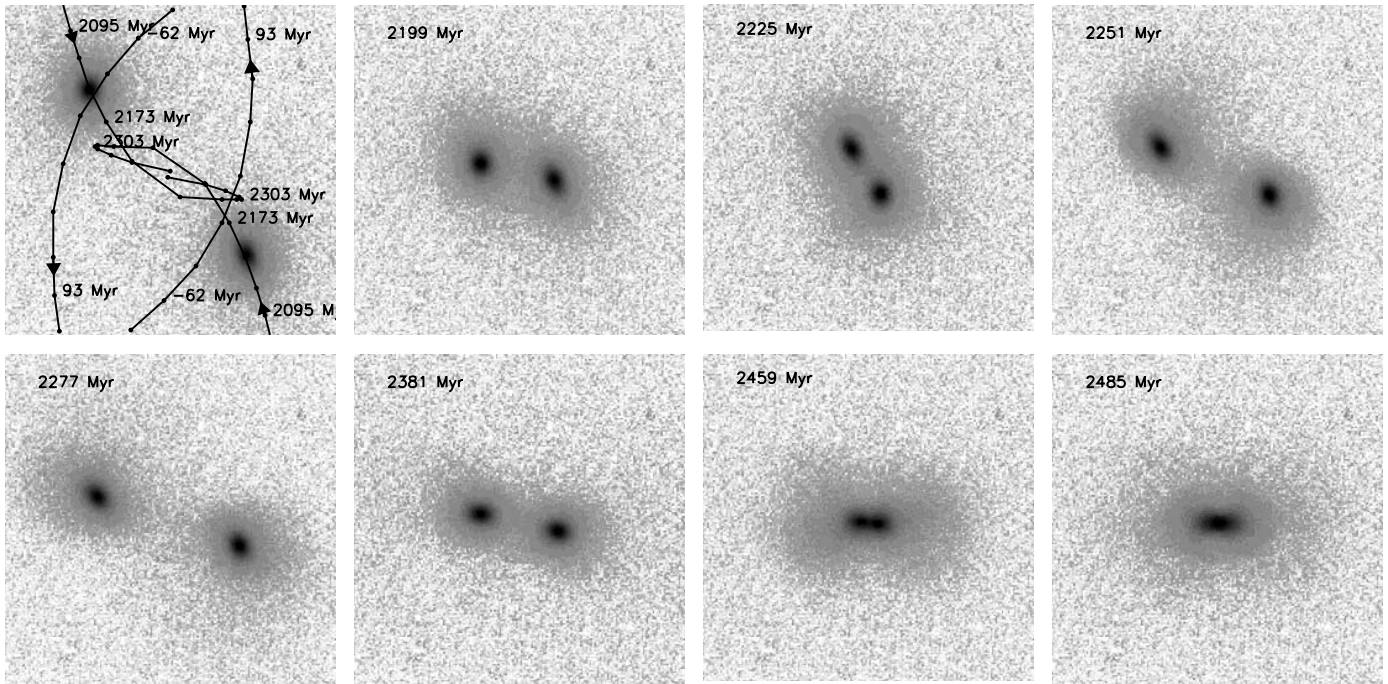


FIG. 1.—Simulation sequence showing the final coalescence of a gas-free elliptical-elliptical 1 : 1 merger. This particular simulation had an initially parabolic orbit with a pericenter of 21 kpc; the face-on projection of the orbital plane is shown in this example. The merger remnant has a final $M_V = -22.5$ and is placed at $z = 0.5$ in real background noise from GEMS with the right size and apparent magnitude. In the first frame, the orbital paths of each galaxy are shown (ticks are every 26 Myr), where a time of 0 corresponds to first pass, 2.21 Gyr to second pass, and final coalescence happens at 2.48 Gyr. The total elapsed time between the first and last frame is 340 Myr, starting 2.15 Gyr after first pass as the galaxies are coming toward second pass (*third frame*) and final coalescence (*last frame*). The images are 50 kpc on a side. This interaction is classifiable as a merger for roughly 200 Myr via either faint and broad tidal features or very close double nuclei.

redshifts, and some may be unbound flyby interactions that will not merge. In order to address these problems, it was necessary to add a second layer of selection. Prolonged experimentation with automated merger diagnostics did not yield satisfactory results and were unable to robustly flag the existence of broad, low surface brightness sheets of debris that are the hallmark of a gas-poor major merger. Therefore, we have used visual classification to screen the automatically selected subsample of close pairs for signs of dry merging. This second level of visual selection is very stringent: in demanding low-level tidal features or very close separations, many merging systems are thrown out of the sample in phases when the tidal features are unobservably weak (simulations suggest this should be the case around $\sim \frac{1}{2}$ of the time). While this reduces the sample size, it provides some measure of security against projections and flybys and results in a smaller but cleaner sample of dry merger candidates (spectroscopy of our dry merger candidates is being sought and will be discussed in future works).

In order to calibrate out and understand the subjectivity of visual classifications, we have adopted a dual strategy: we have visually classified a suite of simulated dry mergers and flybys (selected to have projected separation ≤ 20 kpc) in order to understand better the signatures of a dry merger and to characterize the timescale over which the signs of dry merging are recognizable (§ 3.1), and we use five independent sets of classifications to quantify the degree of reproducibility of dry merger classifications (§ 3.2).

3.1. Expected Morphological Signatures of Dry Mergers

In order to explore the expected appearance of morphological indicators of dry mergers, and the timescales over which these indicators are visible with single-orbit *HST* imaging, we make

use of the simulations of Naab et al. (2006). The progenitors are early-type galaxies and are themselves the remnants of gas-free disk-disk mergers from Naab & Burkert (2003).¹⁴ There are 400,000 particles (160,000 stars and 240,000 dark) per progenitor. A number of simulations with different pericenters and orbital parameters (initially marginally bound, parabolic, or a hyperbolic flyby) were carried out for two mass ratios: 1 : 1 and 3 : 1. A variety of different viewing angles were chosen between face-on and edge-on (with respect to the orbital plane). The simulation output was recorded every 26 Myr. The simulations were used to construct artificial GEMS images; these were created by smoothing to GEMS resolution, rebinning to the appropriate angular diameter distance, and scaling to reproduce a given total luminosity of the remnant. The images were then added to real sky background from GEMS.

From examination of these simulated images (e.g., Fig. 1), some important points become clear. The morphological signatures of interactions between early-type galaxies are often very weak; tidal tails are broad with low surface brightness owing to the high velocity dispersion of the progenitor. Furthermore, there are nearly order-of-magnitude variations in overall merger timescales (i.e., the time from first pass to final coalescence) that depend sensitively on parameters such as mass ratio, pericenter distance, and orbit. Importantly, however, the timescale over which one can recognize tidal features in dry mergers is largely independent of these parameters and is comparable with the galaxies'

¹⁴ Gas-rich major merger remnants are somewhat diskier than remnants from gas-free major disk mergers (Barnes 2002, T. Naab & A. Burkert 2006, in preparation). The adoption of a gas-rich major merger remnant as the spheroidal merger progenitor in what follows does not significantly affect the outcome, while avoiding extra uncertainties associated with the detailed choice of star formation rate and feedback prescriptions.

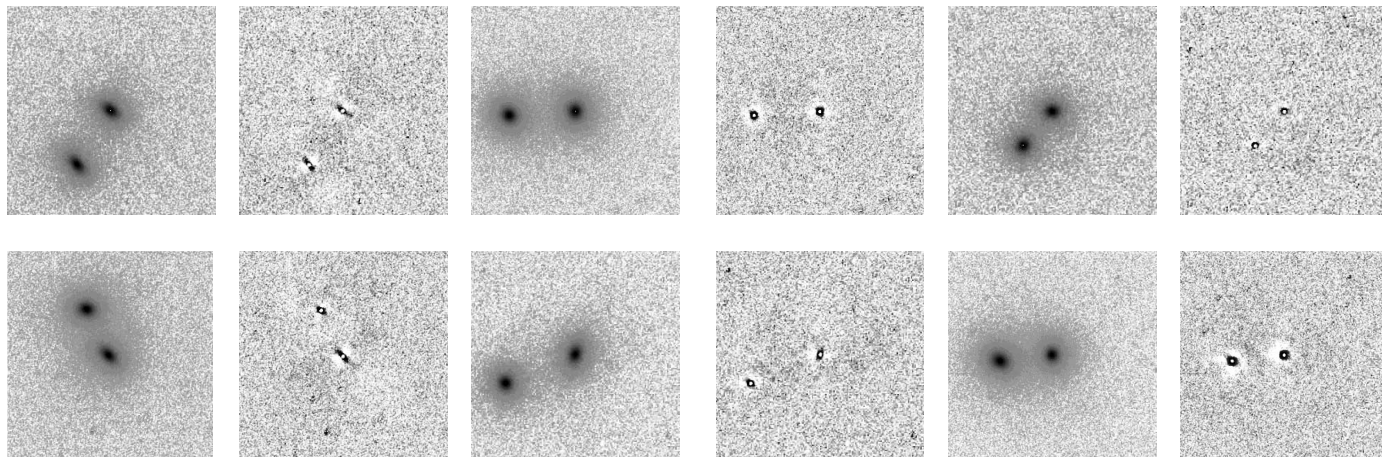


FIG. 2.—Six simulation snapshots deemed to be noninteracting by the majority of the classifiers. We show the simulation and the GALFIT residual side-by-side for each postage stamp. Images are 50 kpc on a side. The residuals in the centers of the galaxies are from small mismatches between the point-spread function (PSF) used to broaden the simulations and the GEMS PSF.

internal dynamical times. Tidal features of sufficient strength to be detected in our images occur only when the galaxies are very close together—typically between the last close pass prior to coalescence and coalescence itself.¹⁵ Orientation plays a role: interactions viewed nearly parallel to the orbital plane are visible as very close pairs for 2–3 times longer than the same interactions viewed from $<60^\circ$ from face-on.

In order to estimate timescales over which GEMS-depth data will be sensitive to dry mergers, we explored the visibility of a wide range of early-type galaxy interactions at a number of redshifts and assuming a range in final merger remnant luminosity. Preliminary explorations showed that luminous dry mergers at $z > 0.7$ are visible only as a very close pair (timescales $\lesssim 50$ Myr, except for rare projections along the orbital plane); the data lack sufficient depth to robustly detect tidal features. Accordingly, we limit this study to $z < 0.7$ galaxies and simulations.

Simulation snapshots were selected randomly from a variety of interaction sequences; the only selection criterion applied was that the nuclei of the galaxies should be separated by <20 kpc (this is an analogous selection to that applied to the data). A total of 174 snapshots from 15 simulations with different mass ratios (1 : 1 and 3 : 1), orbital parameters (marginally bound, parabolic, and a hyperbolic flyby), and viewing angles (viewing angles from 0° from the normal to the orbital plane, 30° , 60° , 80° , and the edge-on 90° orientation) met this separation criterion.¹⁶ The random selection was weighted to ensure that the different viewing angles were selected approximately uniformly in terms of solid angle. Given that a simulation snapshot is created every 26 Myr, this implies that the simulations have two distinct nuclei separated by <20 kpc for on average 300 Myr. The snapshots were scaled to a range of luminosities $M_V < -20.5$ and redshifts $0.1 < z < 0.7$,¹⁷ and a subsample of 25 snapshots were SExtractor,¹⁸ GALFITted, and classified by the five classifiers

(E. F. B., T. N., D. H. M., C. W., and S. K.) in exactly the same way as the data. The classification was blind: simulation snapshots were intermixed with real dry merger candidates from GEMS.

Systems were deemed to be not merging if two classifiers or fewer classified the system as a merger, possibly merging if three classifiers argued it was a merger, and merging if four or five classifiers decided it was a merging system. According to this scheme, 12/25 snapshots were deemed not to be merging, and 13/25 were declared merging (there were no cases in which only three classifiers declared a system to be merging). Examples of each class are shown in Figures 2 and 3. It is apparent that snapshots with very weak/nonexistent tidal features were typically classified as noninteracting, while snapshots with either (1) <5 kpc separation and/or (2) tidal distortions (tails or asymmetries) were classified as interacting. Accordingly, we assign a timescale of $\sim 150 \pm 50$ Myr over which dry mergers are both automatically selected (with separations <20 kpc and timescales ~ 300 Myr) and visually classified as a merger (13/25 of the snapshots, plus associated counting uncertainties).

3.2. Selection of Dry Merger Candidates

The dry merger simulations indicated that dry merger identification is a well-posed problem with quantifiable selection effects for galaxies with $z < 0.7$ and $M_V < -20.5$: at larger redshift and/or fainter limits tidal features are no longer easily visible in single-orbit depth *HST* ACS imaging. Accordingly, we adopt as the parent sample the sample of red-sequence galaxies with $U-V > 1 - 0.31z - 0.08(M_V + 20.77)$, $0.1 \leq z \leq 0.7$, and $M_V < -20.5$ —a sample of 468 galaxies. Galaxy morphologies were assigned by eye for these galaxies: see, e.g., McIntosh et al. (2005), Wolf et al. (2005), or Bell et al. (2004a) for a description of the morphological typing criteria and for some examples from each type. A total of 379/468 galaxies are classified to have early morphological types, E/S0/Sa.¹⁹

Adopting the 468 galaxy red sequence $0.1 \leq z \leq 0.7$ and $M_V < -20.5$ sample as the parent sample, we have selected all close pairs satisfying the following criteria: (1) projected separation <20 kpc, (2) a V -band absolute magnitude difference of

¹⁵ In simulations with small pericenter distances, tidal features are visible for a short time after first pass but become rapidly too weak to observe.

¹⁶ Only one of the flyby snapshots had separation ≤ 20 kpc, reflecting the rapidity of flybys.

¹⁷ The redshifts were drawn from a uniform deviate in terms of volume, not redshift, and are therefore weighted toward higher redshift in exactly the same way as the observational data set (the average redshift of the simulations was 0.53, whereas that of the observational data set is 0.5).

¹⁸ Some very close pairs were deemed to be one object by SExtractor and were therefore fitted with a single Sérsic profile.

¹⁹ Systems with small amounts of ongoing star formation in a weak disk component were allowed into the sample, as long as they were on the red sequence and their light distributions were dominated by a smooth bulge component.

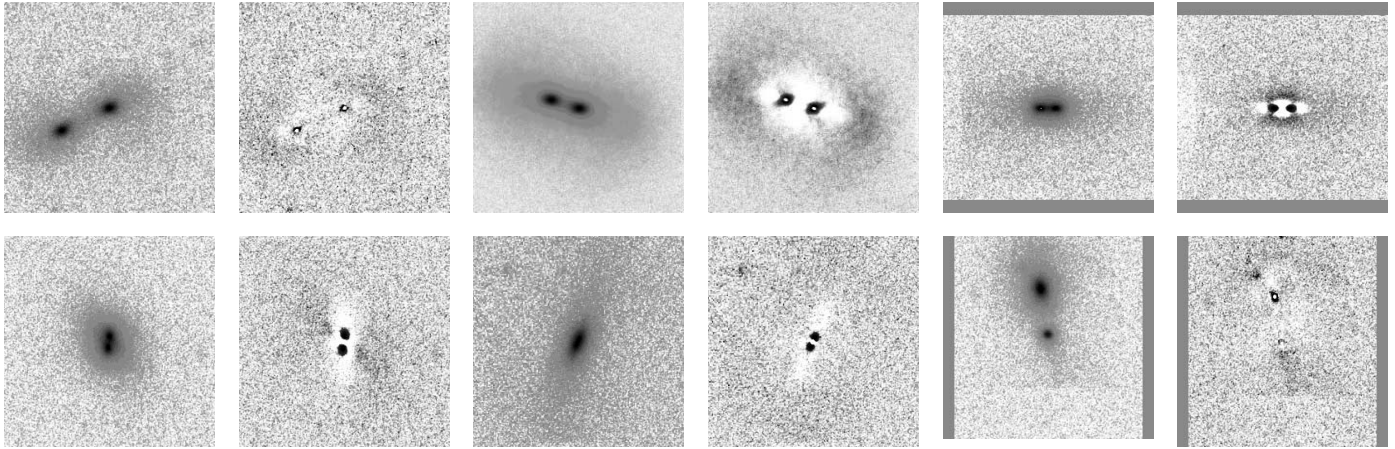


FIG. 3.—Six simulation snapshots deemed to be interacting by the majority of the classifiers. The format is similar to Fig. 2. In all but the top left and bottom right panels, the merging system was determined by SExtractor to be one object and was therefore fitted as one object by GALFIT. There is further discussion of this issue in the text.

1.5 mag or less (corresponding to a 4 : 1 luminosity ratio difference, our threshold for a major merger), and (3) photometric redshift difference $|\Delta z| < 0.1$. Ten pairs were found with these properties.

However, from the visual classifications there were a number of merging systems that were classified by COMBO-17 as one object. It is important to augment the sample of merger candidates with such blended mergers. Every one of the 468 galaxy parent sample has been fitted using the GALFIT galaxy fitting code (Peng et al. 2002) using a single Sérsic profile.²⁰ A sample of 34 galaxies was automatically selected that had strong residuals from the Sérsic profile fit (within one half-light radius, the sum of the absolute values of the residuals exceeded 15% of the total flux within the half-light radius). The vast majority of these 34 systems were bulge/disk systems or had strong dust features and lanes: only six systems had evidence for multiple nuclei. These six systems were added to the sample of 10 COMBO-17-selected close galaxy pairs, forming the final sample of 16 dry

²⁰ The Sérsic (1968) model has a profile with surface brightness $\Sigma \propto e^{-r^{1/n}}$, where r is the radius and n is an index denoting how concentrated the light distribution of a given galaxy is: $n = 1$ corresponds to an exponential light distribution, and $n = 4$ corresponds to the well-known de Vaucouleurs profile.

merger candidates. Postage stamps and GALFIT residuals of all 16 candidates can be found in Figures 4–7.

4. RESULTS

The 16 dry merger candidates were classified by the five classifiers (E. F. B., T. N., D. H. M., C. W., and S. K.), with four different classification categories: (0) no evidence for an interaction, (1) possible merger, (2) dry merger, and (3) gas-rich merger. The results from all classifiers are given in Table 1. On the whole, agreement between the classifiers was good, and the galaxies separated reasonably cleanly into four subsamples: galaxies for which the majority of classifiers felt that there was no evidence for merging (Fig. 4), systems for which classification was uncertain (Fig. 5), gas-rich mergers (Fig. 6), and dry mergers (Fig. 7). A firm classification as a merging system required that four or five classifiers felt that a given system was a definite merger. A total of six systems were identified as dry mergers, three were identified as gas-rich mergers (these systems all had prominent bulge components and red colors), and two of the possible mergers could qualify as a dry merger as both components were bulge-dominated (GEMS 033123.29m274544.9 and GEMS 033313.59m275735.3). Figure 8 shows the color-magnitude diagram of all $0.1 < z < 0.7$ galaxies from COMBO-17 (*points*),

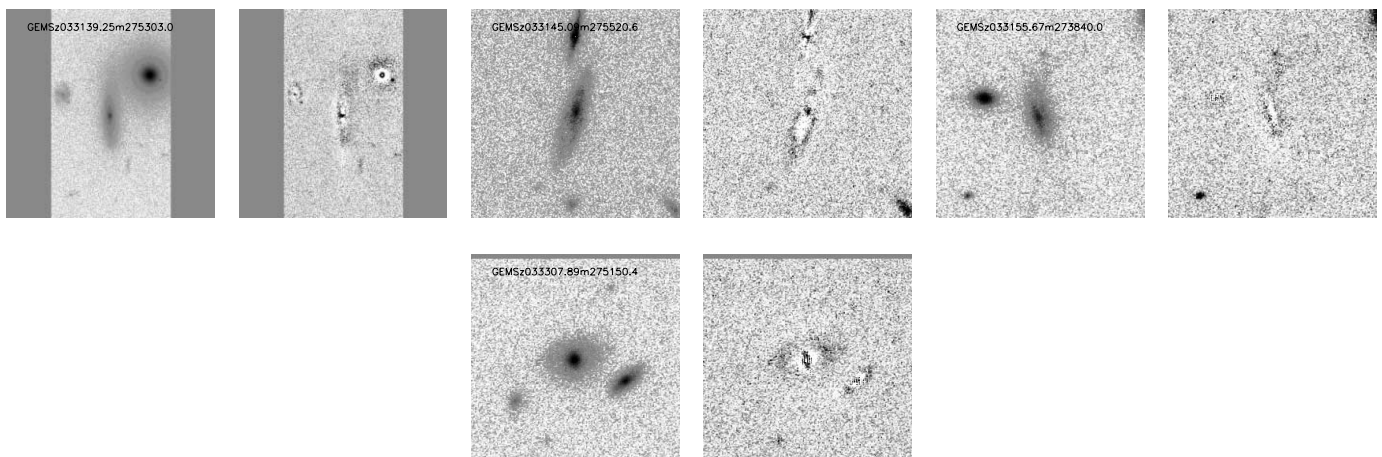


FIG. 4.—Four candidates that were not deemed to be interacting by the majority of the classifiers. We show the image and the GALFIT residual side by side for each sample system. Images are 50 kpc on a side.

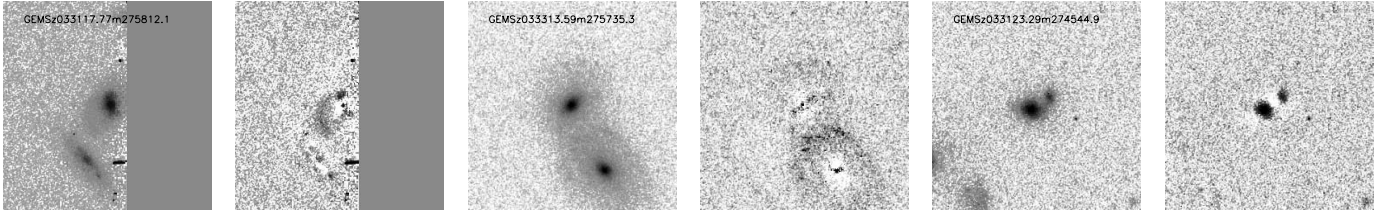


FIG. 5.—Three contentious candidates, arranged in order of decreasing star formation as judged from the classifications. GEMS 033123.29m274544.9 was deemed by SExtractor to be one object and was fitted by GALFIT by a single Sérsic profile.

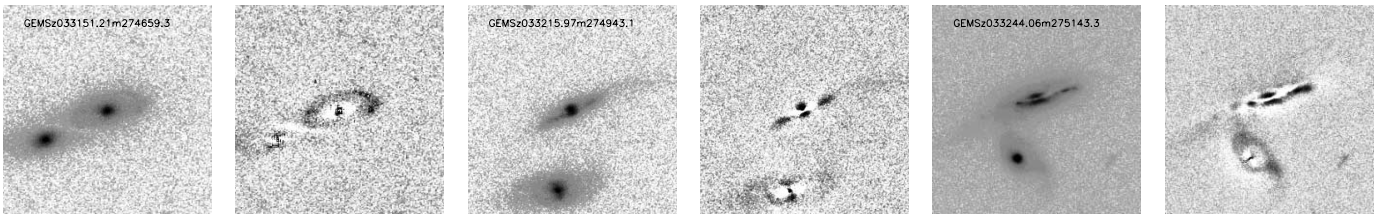


FIG. 6.—Three interactions with clear signs of dust and/or star formation, indicating some gas content. In all cases, both interaction partners have colors consistent with the red sequence (despite often having small amounts of star formation in these systems) and substantial bulge components.

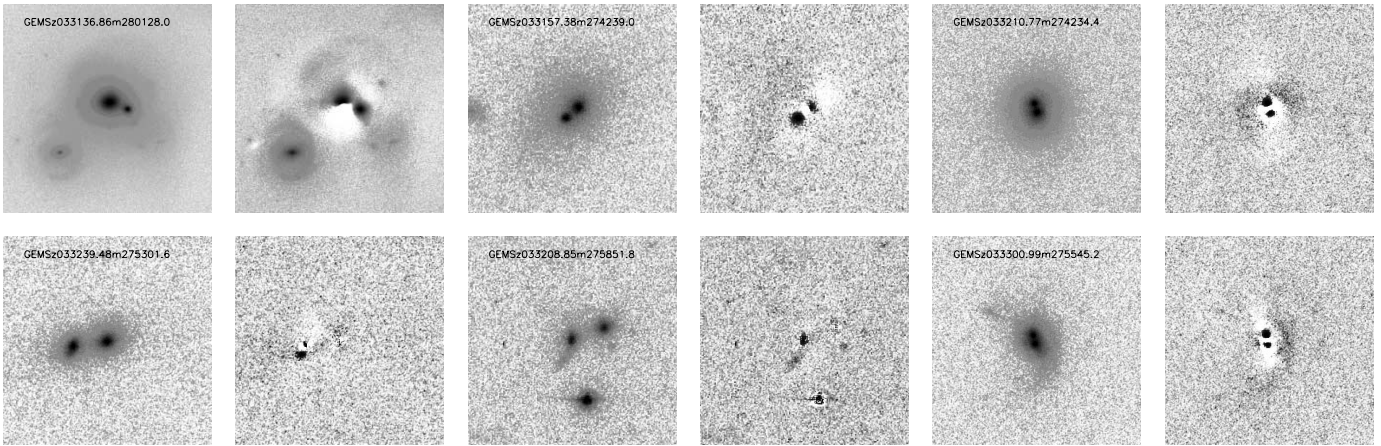


FIG. 7.—Six candidate spheroid-dominated merging systems in GEMS; the last two systems were judged by two out of the five classifiers to have hints of ongoing star formation. Images are 50 kpc on a side. The spiral galaxy in the lower left-hand side of the GEMS 033136.86m280128.0 A and B panel is a background projection. GEMS 033136.86m280128.0, GEMS 033157.38m274239.0, GEMS 033210.77m274234.4, and GEMS 033300.99m275545.2 were deemed by SExtractor to be single objects and were therefore fitted by GALFIT using single Sérsic profiles.

TABLE 1
PROPERTIES OF THE DRY MERGER CANDIDATES

Galaxy Name	R.A.	Decl.	z	M_V	$U-V$	Classification
Galaxies Thought Not To Be Merging						
GEMS 033139.25m275303.0	03 31 39.25	-27 53 03.0	0.20	-21.5	1.1	00000
GEMS 033139.03m275300.1	03 31 39.03	-27 53 00.1	0.20	-21.4	1.3	00000
GEMS 033145.09m275520.6	03 31 45.09	-27 55 20.6	0.49	-20.9	0.9	03003
GEMS 033145.09m275517.4	03 31 45.09	-27 55 17.4	0.57	-20.0	1.0	03003
GEMS 033155.67m273840.0	03 31 55.67	-27 38 40.0	0.519	-20.8	1.2	03300
GEMS 033155.83m273839.4	03 31 55.83	-27 38 39.4	0.526	-20.1	1.2	03300
GEMS 033307.89m275150.4	03 33 07.89	-27 51 50.4	0.518	-21.6	1.3	00003
GEMS 033307.75m275151.2	03 33 07.75	-27 51 51.2	0.44	-20.3	1.0	00003
Contentious Cases						
GEMS 033117.77m275812.1	03 11 17.77	-27 58 12.1	0.58	-21.0	1.0	30303
GEMS 033117.82m275814.1	03 11 17.82	-27 58 14.1	0.55	-20.3	1.0	30303
GEMS 033313.59m275735.3	03 33 13.59	-27 57 35.3	0.66	-23	1.25	20310
GEMS 033313.51m275737.3	03 33 13.51	-27 57 37.3	0.65	-22.5	1.1	20310
GEMS 033123.29m274544.9A	03 31 23.29	-27 45 44.9	0.55	-20.8	0.95	22101
GEMS 033123.29m274544.9B	0.55	-19.3	0.95	22101
Mergers of Galaxies with Significant Bulges and Gas						
GEMS 033244.06m275143.3	03 32 44.06	-27 51 43.3	0.26	-21.7	1.3	33333
GEMS 033244.27m275141.1	03 32 44.27	-27 51 41.1	0.273	-20.5	0.95	33333
GEMS 033215.97m274943.1	03 32 15.97	-27 49 43.1	0.59 ^a	-22.3	1.5	33033
GEMS 033216.16m274941.6	03 32 16.16	-27 49 41.6	0.67	-22.1	0.9	33033
GEMS 033151.21m274659.3	03 31 51.21	-27 46 59.3	0.67 ^b	-22.7	1.0	23333
GEMS 033151.37m274700.3	03 31 51.37	-27 47 00.3	0.64	-21.9	1.2	23333
Galaxies Classified as Dry Mergers by the Majority of Classifiers						
GEMS 033136.86m280128.0A	03 31 36.86	-28 01 28.0	0.15	-22.1	1.5	23222
GEMS 033136.86m280128.0B	0.15	-20.6	1.5	23222
GEMS 033157.38m274239.0A	03 31 57.38	-27 42 39.0	0.62	-22	1.3	22222
GEMS 033157.38m274239.0B	0.62	-22	1.3	22222
GEMS 033208.85m275851.8 ^c	03 32 08.85	-27 58 51.8	0.54	-20.4	1.0	23321
GEMS 033208.76m275851.2 ^c	03 32 08.76	-27 58 51.2	0.54	-20.5	1.0	23321
GEMS 033210.77m274234.4A ^d	03 32 10.77	-27 42 34.4	0.419	-21.9	1.2	22222
GEMS 033210.77m274234.4B ^d	0.419	-21.9	1.2	22222
GEMS 033239.48m275301.6	03 32 39.48	-27 53 01.6	0.65	-22.5	1.25	22221
GEMS 033239.47m275300.5	03 32 39.47	-27 53 00.5	0.65	-21.8	1.2	22221
GEMS 033300.99m275545.2A ^c	03 33 00.99	-27 55 45.2	0.620	-21.7	1.0	23321
GEMS 033300.99m275545.2B	0.620	-21.7	1.0	23321

NOTES.—GEMS galaxy names are simply a combination of their right ascension and declination (where “m” denotes negative declinations), and A and B refer to the two subcomponents when the system was not resolved into two separate galaxies by COMBO-17. Units of right ascension are hours, minutes, and seconds, and units of declination are degrees, arcminutes, and arcseconds. Rest-frame M_V values are approximate and are split using our rough estimate of the luminosity ratio of the merger. Redshifts are accurate to $\delta z \sim 0.02$, magnitudes to ~ 0.2 mag, and colors to ~ 0.15 mag. Redshifts quoted to three significant figures are spectroscopic redshifts from the VIMOS VLT Deep Survey (VVDS; Le Fèvre et al. 2004). See the text for details of the classification scheme.

^a The redshift difference between GEMS 033215.97m274943.1 and GEMS 033216.16m274941.6 is somewhat larger than expected for COMBO-17’s typical redshift error; either one of the redshifts is substantially in error, or our visual classification is inappropriate.

^b The redshift difference between GEMS 033151.37m274700.3 and GEMS 033151.21m274659.3 is consistent with COMBO-17’s redshift error (the galaxies’ visual morphologies show that they are interacting and are therefore at the same redshift).

^c This merger candidate is one COMBO-17 object but was successfully split by the GEMS source extraction algorithm. The coordinates are taken from GEMS, the redshift and color are adopted directly from COMBO-17, and the absolute magnitude of the COMBO-17 object is split into both galaxies using the observed F850LP magnitude ratio from GEMS.

^d GEMS 033210.77m274234.4A and B have been recently discussed in a Keck laser guide star adaptive optics study of mergers detected by *Chandra* (Melbourne et al. 2005, their XID-536; with an X-ray luminosity of nearly 10^{42} ergs s^{-1}). Their luminosities and redshifts are consistent with our own. They fit model SEDs to the observed 0.4–2.2 μm broadband fluxes, concluding that both components are dominated by old stellar populations at the epoch of observation.

^e GEMS 033300.99m275545.2A and B have a COMBO-17 redshift of 0.45; the VVDS redshift is adopted in this paper. Absolute magnitudes and rest-frame colors have been recalculated using the correct VVDS redshift.

all red-sequence early-type galaxies (*gray circles*), and the merger candidates (*black symbols*, where symbol type denotes classification).

On this basis, it is possible to estimate the incidence of major mergers between luminous early-type galaxies from $z \sim 0.7$ to the present day. Among the 379 red, early-type galaxies in GEMS

with $M_V < -20.5$ and $0.1 < z < 0.7$, we find a total of 12 galaxies (six pairs) that are strong dry major merger candidates. Classifications of dry merger simulation snapshots suggest that we will be able to recognize a dry merger for roughly an internal dynamical time, or approximately 150 Myr. Assuming a constant dry merger fraction over the 6.3 Gyr interval $0 < z < 0.7$, an

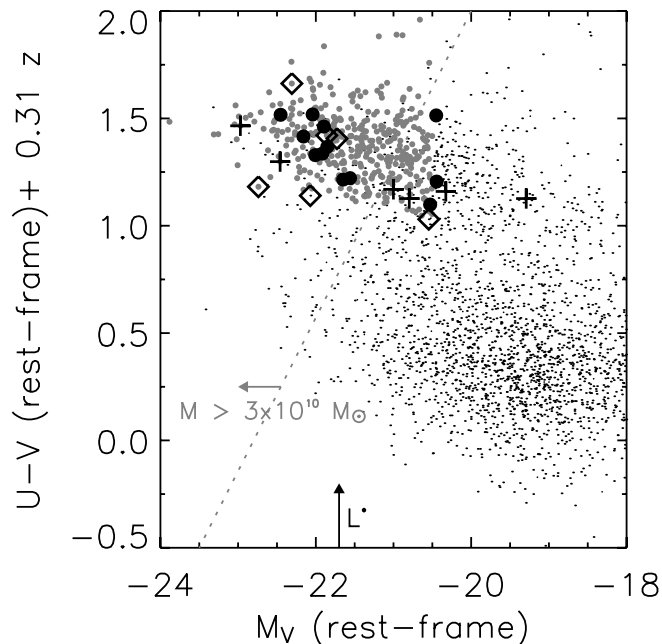


FIG. 8.—Distribution of the candidate spheroid mergers in the color-magnitude diagram. Points denote all galaxies with $0.1 < z < 0.7$; gray circles denote early-type galaxies on the red sequence. Black symbols show possible mergers (*crosses*), gas-rich mergers (*diamonds*), and dry mergers (*filled circles*). In the cases in which COMBO-17 was unable to resolve the merger from the ground and assigned a single redshift, we split the flux between the two galaxies following Table 1 and assign the same color; small random offsets are added to aid visibility. The arrow shows the approximate position of L^* for red-sequence galaxies at $z \sim 0.5$, and the dotted line denotes the locus of galaxies of constant stellar mass $\sim 3 \times 10^{10} M_{\odot}$, assuming a Kroupa (2001) stellar initial mass function.

average, luminous ($M_V < -20.5$) early-type galaxy will undergo $(6.3/0.15)(12/379) \sim 1.3^{+0.7}_{-0.4}$ dry major mergers (with mass ratios between 1 : 1 and 4 : 1). Yet, because there are only six merging pairs, we cannot strongly constrain the merger fraction evolution. The evolution of the merger fraction has been argued to evolve as rapidly as $(1+z)^3$ (e.g., Le Fèvre et al. 2000). If the dry merger fraction were to evolve similarly, an average luminous ($M_V < -20.5$) early-type galaxy will undergo $\sim 0.9^{+0.5}_{-0.3}$ major dry mergers between $z = 0.7$ and the present day. Obviously, our limited number statistics are currently a dominant source of uncertainty; nonetheless, our results indicate that dry merging plays an important role in shaping the properties of luminous early-type galaxies and building up the mass contributed by red-sequence galaxies since $z \sim 1$.

5. DISCUSSION

5.1. Are Our Observations Consistent with Other Observational Constraints?

Is our suggestion that nearly every luminous early-type galaxy in the nearby universe has experienced a major gas-free merger since $z \sim 1$ consistent with existing observational constraints? Dissipationless (=gas-free) merging preserves the fundamental plane (e.g., Nipoti et al. 2003; González-García & van Albada 2003; Boylan-Kolchin et al. 2005); therefore, the thickness of the fundamental plane is not a strong constraint on the prevalence of dry merging. In contrast, simulations and models have demonstrated that dry merging will lead to scatter in the stellar mass–size relation (equivalently, the Kormendy relation; Nipoti et al. 2003) and the color-magnitude relation

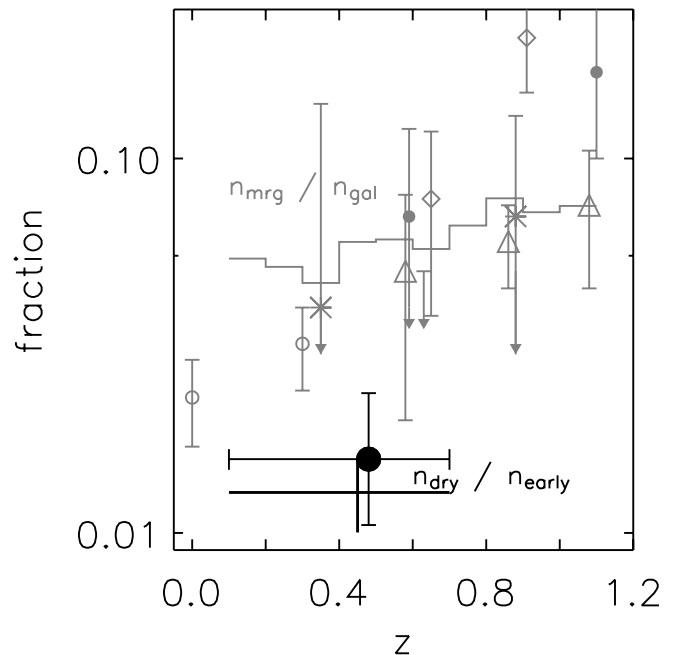


FIG. 9.—Comparison of the dry merger fraction with previous observations of merger fractions and the predictions of a semianalytic model. Gray data points show the merger fraction of galaxies with $M_B \lesssim -20$ from Patton et al. (2002, *open circles*), Le Fèvre et al. (2000, *diamonds*), Conselice et al. (2003, *filled circles*), Lin et al. (2004, *triangles*), and Bundy et al. (2004, *crosses and the upper limit at $z = 0.63$*). The model prediction of the major merger rate for $M_B < -20$ galaxies is shown as a gray line for the redshift range $0.1 < z < 1.1$. The black data point shows the dry merger fraction from this work. The black naked error bar shows the model prediction for the fraction of $M_V < -20.5$ red early-type galaxies that have experienced a major merger in the last 150 Myr averaged over $0.1 < z < 0.7$, with associated number uncertainties.

(CMR; Bower et al. 1998). Observations of the evolution and scatter of these scaling relations limit the amount of dry merging to around a factor of 2 increase in mass since $z \sim 1$ (McIntosh et al. 2005; Bower et al. 1998).²¹ A similar limit is derived from the stellar mass evacuated from the cores of luminous elliptical galaxies by their merging black holes in the absence of gas (Graham 2004).

5.2. Comparison with Previous Measurements of Merger Fraction

It is interesting to compare our results with previous observational estimates of the overall galaxy merger fraction. In Figure 9, we show the dry merger fraction (*black filled circles*) of $M_V < -20.5$ red early-type galaxies, along with the fraction of $M_B \lesssim -20$ galaxies in close pairs with ≤ 20 kpc separation taken from Le Fèvre et al. (2000, *open diamonds*) and Patton et al. (2002, *open circles*). The results for Lin et al. (2004) are shown as triangles (separations between 10 and 30 kpc; $M_B \lesssim -20$). Bundy et al. (2004) argued that many close pairs with nearly equal optical magnitudes were minor mergers in which the satellite galaxies had boosted optical flux from tidally induced bursts of star formation; they used near-infrared photometry to estimate the major merger fraction (*crosses*, and the upper limit at $z = 0.63$). The filled circles denote the merger fraction of $M_B < -20$ galaxies, inferred using morphological disturbance as an indicator of past merging activity (Conselice et al. 2003).

²¹ The CMR limit applies since the epoch when the CMR was imprinted on the early-type galaxy population.

It is clear that the dry merger fraction is lower than the general merger fraction. A number of factors may contribute to this reduction. Close pairs and morphologically selected gas-rich mergers are expected to be visible for a timescale $\tau \sim 0.5\text{--}1$ Gyr (Le Fèvre et al. 2000; Patton et al. 2002; Conselice et al. 2003), whereas dry mergers are visible for $t_{\text{dry}} \sim 150$ Myr. Episodes of star formation in gas-rich mergers will increase the brightness of the merging galaxies, increasing their prominence relative to the star formation-free dry mergers. Finally, gas-rich galaxies tend to inhabit lower density environments than gas-poor galaxies; this difference in environment will also affect the likelihood of a major merger.

5.3. Theoretical Expectations in a Hierarchical Universe

Do hierarchical models predict that dry mergers are an important mode of transformation and mass growth for luminous elliptical galaxies? To address this question, we make use of an updated version of the Somerville et al. semianalytic galaxy formation model (see Somerville & Primack [1999]; Somerville et al. [2001], for a description of the basic ingredients), based in the standard Λ CDM paradigm of hierarchical structure formation. The models are based on Monte Carlo realizations of dark matter halo merger histories, constructed using the method described in Somerville & Kolatt (1999), and include fairly standard recipes treating gas cooling, star formation, and supernova feedback. The star formation rate is given by $\dot{m}_* = m_{\text{cold}}/(\tau_*^0 t_{\text{dyn}})$, where m_{cold} is the cold gas mass in the galaxy, t_{dyn} is the dynamical time of the disk, and τ_*^0 is a free parameter, which is adjusted to obtain agreement with observed gas fractions in spiral galaxies at the present day. We convolve the resulting star formation histories with the multimetallicity stellar spectral energy distribution (SED) models of Bruzual & Charlot (2003) and include the effects of dust extinction using a simple relationship between face-on B -band optical depth and star formation rate ($\tau_B \propto \text{SFR}^\beta$); based on the observational results of Wang & Heckman (1996), we assume $\beta = 0.5$. Merging of galaxies (substructure) within virialized dark matter halos is tracked by computing the time it takes for a satellite galaxy to lose all of its orbital angular momentum via dynamical friction against the background of the dark matter halo, using the standard Chandrasekhar approximation. Mergers with mass ratio 1:4 or greater are assumed to result in a burst of star formation, and all preexisting “disk” stars are transferred to a “bulge” component.

Earlier versions of this model, like many other models in the literature, had difficulty producing enough luminous red galaxies, particularly at high redshift (see, e.g., Somerville et al. 2004), and therefore could not produce a useful prediction of the merger rate for these systems. R. Somerville et al. (2006, in preparation) find that introducing an ad hoc “quenching” of star formation when the mass of the bulge component grows larger than $M_{\text{bulge, crit}} \simeq 2 \times 10^{10} M_\odot$ leads to much improved agreement with the observed $0 < z \lesssim 1$ color distributions as a function of absolute magnitude, including the observed bimodality of the color distributions at $z \sim 0\text{--}2$. A full description of this model will be presented in this forthcoming work: at this stage, we argue that as the model approximately reproduces the global luminosity functions and observed number of red, early-type galaxies at $z \sim 0\text{--}1$, it is at least a useful starting point to examine the overall merger rate and the dry merger rate.

In Figure 9, we show the predicted fraction of $M_B \lesssim -20$ galaxies that have experienced a major merger within the past 1 Gyr (*gray line*; major mergers are defined as having mass ratios between 1:1 and 4:1). These predictions are derived from a mock light cone from $0.1 < z < 1.1$ covering a sky area of

1 deg² (corresponding to about 4 times the volume of GEMS). Bearing in mind on one hand the difficulties of measuring galaxy merger rate from close pairs, and on the other hand uncertainties in physical prescriptions for dynamical friction, tidal stripping of galaxy halos, and tidally induced star formation, the agreement between the model and observations is rather good. There is a hint that the model merger fraction decreases rather less rapidly than the observations; interestingly, this behavior is also seen in the semianalytic models of Benson et al. (2002), as shown in Figure 13 of Conselice et al. (2003).

The black naked error bar shows the dry merger fraction predicted by this model. We identify dry mergers in the model as galaxies with magnitudes $M_V < -20.5$, $U\text{--}V$ colors on the red sequence, and that have had a major merger in the past 150 Myr. The mock catalog has roughly 4 times the volume of GEMS; there are 13 merging systems from 982 early-type $M_V < -20.5$ red-sequence galaxies in this mock catalog in the interval $0.1 < z < 0.7$. The inferred merger fraction is in excellent quantitative agreement with our observational determination (six systems from 379 galaxies). This result lends further theoretical support to hydrodynamic studies of elliptical galaxy formation (Dominguez-Tenreiro et al. 2004) and semianalytic studies of galaxy clusters (Khochfar & Burkert 2003), both of which argue that dry mergers are an important process in driving the buildup of massive early-type galaxies at recent times.

6. CONCLUSIONS

We have used the GEMS and COMBO-17 surveys in conjunction with N -body and semianalytic galaxy formation simulations to explore the frequency of gas-free major mergers between spheroid-dominated galaxies (dry mergers) since $z = 0.7$. We focused on this aspect of galaxy merging, both because identifying gas-free mergers is less likely to be complicated by the effects of merger-induced star formation and the accompanying dust extinction and because it can be modeled relatively straightforwardly (for similar reasons). The morphological signatures of such interactions were calibrated using mock GEMS-like images based on N -body simulations and include < 5 kpc separation of close nuclei and/or broad tidal tails and asymmetries. The simulations showed that such features are visible only for galaxies with $M_V \lesssim -20.5$ in single-orbit *HST* F850LP data at $z \lesssim 0.7$; higher redshift galaxies show unobservably weak tidal features in the GEMS data. A total of 809 red-sequence galaxies were visually inspected for morphological signatures of spheroid merging; six systems (12 galaxies) with luminosity ratios between 1:1 and 4:1 were found out of a total of 379 red-sequence early-type galaxies with $M_V < -20.5$. The simulations suggest that morphological signatures of spheroid merging are visible for ~ 150 Myr; we therefore argue that an average $M_V < -20.5$ early-type galaxy has experienced between 0.5 and 2 major spheroid mergers since $z \sim 0.7$. This merger frequency is consistent with limits of $\lesssim 1$ major gas-free merger at recent times, as derived from the color-magnitude and stellar mass-size relations, and from core mass deficits. We have compared this result with an updated semianalytic model. This model reproduces the evolution of the number of luminous red early-type galaxies and the overall merger fraction reasonably well and can therefore be used to obtain a plausible prediction of the frequency of dry mergers in a hierarchical universe. The predicted dry merger fraction is consistent with the observations to within their combined uncertainties. Thus, both observations and theory lend strong support to the notion that major spheroid mergers are an important driver of the evolution of luminous early-type galaxies in recent epochs.

We wish to thank the referee for a number of helpful suggestions. E. F. B. wishes to thank Ralf Bender and Marijn Franx for interesting discussions. Based on observations taken with the NASA/ESA *Hubble Space Telescope*, which is operated by the Association of Universities for Research in Astronomy, Inc., under NASA contract NAS5-26555. Support for the GEMS project was provided by NASA through grant GO-9500 from the Space

Telescope Science Institute. E. F. B. was supported by the European Community's Human Potential Program under contract HPRN-CT-2002-00316 (SISCO). S. J. and D. H. M. acknowledge support from NASA under LTSA grant NAG5-13063 and NAG5-13102, respectively. C. W. was supported by a PPARC Advanced Fellowship. K. J. was supported by the German DLR under project 50 OR 0404. C. H. acknowledges financial support from the GIF.

APPENDIX

ARE FLYBYS IMPORTANT?

Tran et al. (2005) recently showed that all luminous dry merger candidates in the outskirts of the $z \sim 0.8$ MS 1054 galaxy cluster with a sufficient signal-to-noise ratio to measure velocity offsets were indeed bound ($R < 10$ kpc) pairs (with velocity differences less than 200 km s^{-1}). Noting that Tran et al. (2005) and van Dokkum et al. (1999) argue that most of these galaxies are in the cluster infall region (and therefore are in group environments that are about to be incorporated into the cluster proper), their study supports the notion that the majority of the dry merger candidates studied in this paper are bound and will likely merge.

Yet, one of the few published examples of an elliptical-elliptical interaction in the local universe (NGC 4782/4783) has been shown by Madejsky et al. (1991) to have an unbound hyperbolic orbit. Based on simulated images from simulations of unbound dry mergers similar to those discussed in the main text, we find that morphological disturbances generated by flyby interactions are short-lived, $\ll 50$ Myr for systems of a similar luminosity to the ones we observe here. Nonetheless, if the number of flyby interactions is much larger than the number of mergers, flybys could significantly contaminate a spheroid major merger sample.

Because galaxies with velocity differences greatly in excess of their internal velocity dispersion are extremely unlikely to merge, it is worth understanding the likely contribution of high-velocity flybys to tidally disturbed spheroid-dominated systems in a cosmic-averaged sense. The relative velocity difference is a strong function of the velocity dispersion of the local environment. We explore the likelihood of producing a given tidal effect in different environments by adopting the impulse approximation. We wish to work out the number of interactions as a function of environment, characterized by the velocity dispersion of the local environment σ . The number of interactions $N_{\text{int}} \propto n_{\text{E/S0}}^2 r^2$, where $n_{\text{E/S0}}$ is the number density of E/S0 galaxies and r is the pericentric distance. The dependence of cross section on velocity can be estimated by assuming that the relative velocity $v \propto \sigma$. In order to work out the cross section for interaction producing a given displacement in stars s as a function of v , we note that tidal forces $F \propto r^{-3}$. Since the interaction timescale $t \propto 1/v$, the displacement in stars $s \propto Ft^2 \propto r^{-3}v^{-2}$. Thus, given a constant tidal displacement of stars s , the impact parameter $r \propto v^{-2/3}$. The number of E/S0 galaxies can be estimated assuming a constant group stellar M/L ; $n_{\text{E/S0}} \propto f_{\text{E/S0}} M_{\text{halo}} / r_{\text{halo}}^3$. Since $M_{\text{halo}} \propto \sigma^3$ and $r_{\text{halo}} \propto \sigma$, $n_{\text{E/S0}} \propto f_{\text{E/S0}}$ alone; we assume for simplicity $f_{\text{E/S0}} \propto \sigma \propto v$. Thus, $N_{\text{int}} \propto v^{2/3}$. To estimate the fraction of galaxies with this given displacement of stars owing to tidal effects, f_{int} , one divides by the total number of E/S0 galaxies $N_{\text{E/S0}} \propto f_{\text{E/S0}} M_{\text{halo}} \propto v^4$; thus, $f_{\text{int}} \propto v^{-10/3}$. A cosmic-averaged fraction must be further weighted by the halo mass function of group and cluster-sized halos, $\Phi(\sigma) \propto \sigma^{-3}$. Thus, despite the dominance of E/S0 galaxies in clusters, the vast majority of tidally disturbed spheroid-dominated galaxies are in the lowest velocity dispersion groups capable of hosting E/S0 galaxies and are therefore likely to merge.

A complementary analysis following Makino & Hut (1997) asking what the average environment of spheroid mergers should be (using the scalings above) comes to a similar conclusion, $f_{\text{mrg}} \propto 1/\sigma^2$, and weighting by the mass function of groups and clusters, the cosmic-averaged fraction is again completely dominated by low-speed E/S0 mergers in low-mass groups.

REFERENCES

- Barnes, J. E. 2002, *MNRAS*, 333, 481
 Barnes, J. E., & Hernquist, L. 1996, *ApJ*, 471, 115
 Bell, E. F., et al. 2004a, *ApJ*, 600, L11
 ———. 2004b, *ApJ*, 608, 752
 Bender, R. 1988, *A&A*, 202, L5
 Bendo, G. J., & Barnes, J. E. 2000, *MNRAS*, 316, 315
 Benson, A. J., Lacey, C. G., Baugh, C. M., Cole, S., & Frenk, C. S. 2002, *MNRAS*, 333, 156
 Bower, R. G., Kodama, T., & Terlevich, A. 1998, *MNRAS*, 299, 1193
 Boylan-Kolchin, M., Ma, C.-P., & Quataert, E. 2005, *MNRAS*, 362, 184
 Bruzual, G., & Charlot, S. 2003, *MNRAS*, 344, 1000
 Bundy, K., Fukugita, M., Ellis, R. S., Kodama, T., & Conselice, C. J. 2004, *ApJ*, 601, L123
 Chen, H.-W., et al. 2003, *ApJ*, 586, 745
 Conselice, C. J., Bershad, M., Dickinson, M., & Papovich, C. 2003, *AJ*, 126, 1183
 Conselice, C. J., Blackburne, J. A., & Papovich, C. 2005, *ApJ*, 620, 564
 Cross, N. J. G., et al. 2004, *AJ*, 128, 1990
 de Lucia, G., et al. 2004, *ApJ*, 610, L77
 Domínguez-Tenreiro, R., Sáiz, A., & Serna, A. 2004, *ApJ*, 611, L5
 Drory, N., Bender, R., Feulner, G., Hopp, U., Maraston, C., Snigula, J., & Hill, G. J. 2004, *ApJ*, 608, 742
 Faber, S. M., et al. 1997, *AJ*, 114, 1771
 ———. 2006, *ApJ*, submitted (astro-ph/0506044)
 Ford, H., et al. 2003, *Proc. SPIE*, 4854, 81
 González-García, A. C., & van Albada, T. S. 2003, *MNRAS*, 342, L36
 Graham, A. 2004, *ApJ*, 613, L33
 Khochfar, S., & Burkert, A. 2003, *ApJ*, 597, L117
 ———. 2005, *MNRAS*, 359, 1379
 Kodama, T., et al. 2004, *MNRAS*, 350, 1005
 Kormendy, J., & Bender, R. 1996, *ApJ*, 464, L119
 Kroupa, P. 2001, *MNRAS*, 322, 231
 Kuntschner, H. 2000, *MNRAS*, 315, 184
 Lauer, T. R., et al. 1995, *AJ*, 110, 2622
 Le Fèvre, O., et al. 2000, *MNRAS*, 311, 565
 ———. 2004, *A&A*, 428, 1043
 Lin, L., et al. 2004, *ApJ*, 617, L9
 Madejsky, R., Bender, R., & Möllenhoff, C. 1991, *A&A*, 242, 58
 Makino, J., & Hut, P. 1997, *ApJ*, 481, 83
 McIntosh, D. H., et al. 2005, *ApJ*, 632, 191
 Melbourne, J., et al. 2005, *ApJ*, 625, L27
 Naab, T., & Burkert, A. 2001, in *ASP Conf. Ser. 249, The Central Kiloparsec of Starbursts and AGN: The La Palma Connection*, ed. J. H. Knapen et al. (San Francisco: ASP), 735
 ———. 2003, *ApJ*, 597, 893
 Naab, T., Burkert, A., & Hernquist, L. 1999, *ApJ*, 523, L133
 Naab, T., Khochfar, S., & Burkert, A. 2006, *ApJ*, 636, L81
 Nipoti, C., Londrillo, P., & Ciotti, L. 2003, *MNRAS*, 342, 501
 Patton, D. R., et al. 2002, *ApJ*, 565, 208
 Peng, C. Y., Ho, L. C., Impey, C. D., & Rix, H.-W. 2002, *AJ*, 124, 266

- Rix, H.-W., et al. 2004, *ApJS*, 152, 163
Saracco, P., et al. 2005, *MNRAS*, 357, L40
Sérsic, J. L. 1968, *Atlas de Galaxies Australes* (Cordoba: Observatorio Astronomico)
Somerville, R. S., & Kolatt, T. S. 1999, *MNRAS*, 305, 1
Somerville, R. S., & Primack, J. R. 1999, *MNRAS*, 310, 1087
Somerville, R. S., Primack, J. R., & Faber, S. M. 2001, *MNRAS*, 320, 504
Somerville, R. S., et al. 2004, *ApJ*, 600, L135
Thomas, D., Maraston, C., Bender, R., & Mendes de Oliveira, C. 2005, *ApJ*, 621, 673
Trager, S. C., Faber, S. M., Worthey, G., & González, J. J. 2000, *AJ*, 120, 165
Tran, K.-V. H., van Dokkum, P., Franx, M., Illingworth, G. D., Kelson, D. D., & Förster Schreiber, N. M. 2005, *ApJ*, 627, L25
Toomre, A., & Toomre, J. 1972, *ApJ*, 178, 623
van der Wel, A., Franx, M., van Dokkum, P. G., & Rix, H.-W. 2004, *ApJ*, 601, L5
van Dokkum, P. G., Franx, M., Fabricant, D., Kelson, D. D., & Illingworth, G. D. 1999, *ApJ*, 520, L95
Wang, B., & Heckman, T. 1996, *ApJ*, 457, 645
Wolf, C., et al. 2004, *A&A*, 421, 913
———. 2005, *ApJ*, 630, 771